

# Structural aspects of the interaction of mannan-based polysaccharides with bacterial cellulose

Sarah E. C. Whitney<sup>a</sup>, Jennie E. Brigham<sup>a</sup>, Arthur H. Darke<sup>a</sup>,  
J. S. Grant Reid<sup>b</sup>, Michael J. Gidley<sup>a,\*</sup>

<sup>a</sup>Unilever Research Laboratory, Colworth House, Sharnbrook, Bedfordshire, UK, MK44 1LQ

<sup>b</sup>Department of Biological and Molecular Sciences, University of Stirling, Stirling, UK, FK9 4LA

Received 6 August 1997; accepted 12 December 1997

---

## Abstract

Interactions between cellulose and glucomannan/galactomannans have been studied through molecular and ultrastructural analysis of composites formed by deposition of cellulose from *Acetobacter aceti* ssp. *xylinum* into solutions containing either glucomannan or galactomannans of varying Man:Gal ratio. <sup>13</sup>C NMR suggests that unsubstituted mannan segments can bind to cellulose by undergoing a conformational transition to an extended 2-fold form. Konjac glucomannan induces a coalescence of cellulose fibrils and a dramatic reduction of crystallinity: low galactose galactomannans also show these trends. The inferred mannan/cellulose sandwich structure may underlie the densification processes which can accompany mannan-containing secondary cell wall formation. Medium galactose galactomannans additionally form cross-links of varying lengths between cellulose fibrils and show evidence for self-association. The presence of cellulose fibrils promotes network formation from galactomannan solutions under conditions where this would not normally occur. The principles of interaction between cellulose and mannan-based polymers at both molecular and ultrastructural levels are discussed in the context of plant cell wall design and assembly. © 1998 Elsevier Science Ltd. All rights reserved

**Keywords:** Cellulose/mannan interactions; Glucomannan; Galactomannan; *Acetobacter aceti*; Plant cell wall assembly

---

## 1. Introduction

Mannan-based polysaccharides are found extensively throughout nature as major components of plant cell walls. Nearly pure mannan, a homopolymer of (1→4)-linked  $\beta$ -D-Manp, has been identified in ivory nut, date, palm and coffee bean

endosperms [1]. Crystalline mannan microfibrils act as a functional replacement for cellulose in siphonous green algae of the families *Codiaceae* and the *Dasycladaceae* [2]. Glucomannan, in which a number of the mannose residues are replaced by  $\beta$ -(1→4)-linked Glc, is a major hemicellulose in hardwoods and is found in a number of roots, tubers and bulbs, as well as a few seed types [1]. Galactomannans, in which the  $\beta$ -(1→4)-linked mannan backbone is substituted at C-6 with  $\alpha$ -D-Gal [3],

---

\* Corresponding author.

form major storage polysaccharides in leguminous seeds. A model for galactomannan biosynthesis, which incorporates the taxonomically important Man:Gal variability between species has been proposed [4,5]. Mannan-based polysaccharides are also often found as components in Type I [6] primary cell walls. Examples include tomato fruit [7], runner beans [8] and potato tubers [9].

In addition to their botanical importance, mannans have widespread applications as gelling agents and stabilisers in the food industry. Konjac glucomannan can be induced to form gels after deacetylation by alkali treatment [10]. Intermolecular associations between galactomannans occur in water. The degree of association is increased as galactose content decreases [11–13] and is alkali-sensitive [14], implying that association is via an unsubstituted mannan backbone. Both polymers can modify the gelling properties of certain polysaccharides. Mixtures of mannan-based polysaccharides with non-gelling polymers can promote gel formation [15–18] under conditions in which neither polymer in isolation will gel. Gel strength and stability of gelling polysaccharides can be significantly increased in the presence of gluco- or galactomannans [19,20].

Although mannan-based polysaccharides are components of most cell wall types, their role in both the ultrastructure and molecular organisation of the wall is unclear. As major hemicellulosic components, an intimate association with cellulose in cellulose-based walls is predicted, but the molecular and ultrastructural aspects of the interaction have not been comprehensively explored.

The Gram negative bacterium *Acetobacter aceti* ssp. *xylinum* synthesises pure, highly crystalline cellulose I as an extracellular polysaccharide. Cellulose ribbon synthesis and assembly occurs as a cell directed hierarchical process and can be interrupted by the addition of fluorescent brighteners and polysaccharides [21–23]. Addition of hemicelluloses to a fermentation medium containing *A. aceti* has been shown to facilitate cellulose-hemicellulose interaction [24,25]. If high molecular weight tamarind xyloglucan is added, composite networks are formed which closely resemble, at the ultrastructural and molecular level, cellulose-xyloglucan networks found in Type I cell walls [26–28]. The *Acetobacter* system has been proposed as a good model for cell wall assembly processes [26].

Interactions between mannan and cellulose are predicted as pure mannan shows similarities to

cellulose in terms of stereochemistry, differing only in configuration at O-2 which is axial in Man, but equatorial in Glc. Highly crystalline cellulose microfibrils can be used as the substrate for co-crystallisation of mannan to form “shish-kebab” structures, in which mannan adopts a two-fold screw conformation closely matching that of cellulose [29]. In studies of synergistic interactions between galactomannans and other polysaccharides, the relative Man content of galactomannan has been shown to be positively correlated with degree and strength of association [13,19]. It might therefore be predicted that Man:Gal ratio will affect the level of interaction with cellulose. However, no evidence for this hypothesis is obtained from X-ray diffraction, as the crystal lattice constants of pure mannan [2] are similar to those of galactomannan gums [30,31]. Crystal and molecular structure is therefore independent of Man:Gal ratio under the conditions used to produce films and fibres for diffraction studies. Similarly, glucomannans of varying Man:Glc ratios have mannan I crystal structures with relatively invariant lattice parameters [29]. This might suggest that the ability of gluco- and galactomannans to bind to cellulose may not be strictly dependent on Man:Gal/Glc ratios. <sup>13</sup>C NMR studies however show that conformations characteristic of crystalline mannan are not present in solutions or gels of either glucomannans or galactomannans [32], suggesting that the crystal structures previously obtained do not persist under highly hydrated conditions.

This paper describes ultrastructural and molecular aspects of cellulose composites formed by the addition of gluco- and galactomannans to the *Acetobacter* system. Galactomannans isolated from various sources can be used to investigate the effect of varying Man:Gal ratio. High Gal galactomannans are sourced from guar (*Cyamopsis tetragonoloba*) and fenugreek (*Trigonella foenum-graecum*) which have Man:Gal ratios of 1.6 and 1.1, respectively. The commercially available galactomannan from *Ceratonia siliqua* (Locust Bean Gum (LBG)), has a Man:Gal ratio of ca. 3.5, but it can be separated, on the basis of differential solubility, into galactomannan sub-fractions ranging in Man:Gal ratio from 5.5 to 2.5. The availability of galactomannans differing in their Man:Gal ratio allows an examination of the contributions of residue types to the interaction of mannan-based polysaccharides with cellulose.

## 2. Experimental

**Purification of polysaccharides.**—Konjac glucomannan was purified from Konyaku flour. 12 g flour was added slowly to 1.0 L deionised water (containing 0.05%  $\text{NaN}_3$ ) and extracted at 80 °C with overhead stirring for 2 h. After centrifugation at 27,500 g for 20 min at 4 °C the supernatant was decanted. The pellet was resuspended in 500 mL deionised water and extracted as above. The supernatants were combined, dialysed against deionised water for 1 week at 1 °C and subsequently freeze-dried.

Locust bean gum fractions were prepared by extraction of commercial LBG (RL 200, Meyhall, Switzerland) under various temperature regimes. Commercial material (15 g) was dissolved in 1500 mL deionised water and stirred using a Silverson mixer for 90 min at 25 °C. Dissolved material was collected by centrifugation (27,500 g, 30 min, 4 °C). The supernatant was decanted and the pellet suspended in 750 mL deionised water for extraction at 45 °C. A final extraction was performed at 80 °C and the insoluble residue discarded. Fractionated samples are designated LBG<sub>25</sub>, LBG<sub>25–45</sub> and LBG<sub>45–80</sub> respectively. High molecular weight material was precipitated from the three supernatants in 2:1 iso-propyl alcohol (IPA)/water at room temperature. Precipitated material was washed in pure IPA and soaked in acetone overnight. The acetone was removed by vacuum filtration and the precipitate dried further in a vacuum oven at 40 °C for 24 h. Unfractionated LBG (LBG<sub>uf</sub>) was prepared as above, but with a single extraction at 75 °C.

Guar gum was from a commercial source (Hercules, USA). Fenugreek galactomannan was purified according to the method described by Campbell and Reid [33].

All mannan-based polysaccharides were of high molecular weight as evidenced by intrinsic viscosities of 5–10 dL/g and high solution viscosities at low concentrations.

**Fermentation cultures.**—Control incubations of *Acetobacter aceti* ssp. *xylinum* (ATCC 53524) in Hestrin Schramm medium pH 6.2 [34] containing 2% Glc or experimental incubations which additionally contained 0.2% or 0.5% LBG fractions or 0.5% Konjac glucomannan were performed at 30 °C, 50 rpm for 2 days, essentially as described by Whitney et al. [26]. Each incubation was replicated three times. After incubation, cellulosic material

was removed and washed in many changes of ice-cold sterilised deionised water. Samples were stored in 0.02%  $\text{NaN}_3$  at 1 °C.

**Deep-etch, freeze-fracture transmission electron microscopy.**—The molecular architecture of cellulose/mannan samples was determined by high resolution microscopy exactly as described by Whitney et al. [26].

**Monosaccharide analysis.**—Polysaccharide samples were hydrolysed in 12 M  $\text{H}_2\text{SO}_4$  for 1 h at 35 °C, followed by 3 h at 100 °C in 1 M  $\text{H}_2\text{SO}_4$ . Hydrolysed material was converted to alditol acetates according to the method of Blakeney et al. [35] and separated on a Carlo Erba HRGC 5300 with an SP-2330 fused silica capillary column (30 m×0.25 mm id) held at 230 °C for 40 min and detected using a flame ionisation detector. In the absence of added mannans, only glucose was detected indicative of the purity of the bacterial cellulose.

**NMR spectroscopy.**—NMR spectra of composites were obtained as described by Whitney et al. [26]. Wet samples (300–400 mg, ca. 90% water) were studied; acquisition times were 1 s, relaxation delays 4 s and total experimental times were typically 16–24 h.

## 3. Results

**Composites formed with Konjac glucomannan.**—Significant incorporation of Konjac glucomannan into composites is seen, with a cellulose:glucomannan ratio of ca. 1:0.59 (Tables 1 and 2), slightly higher than the results obtained by Hackney et al. [25] for a similar system.

In the absence of modifying polysaccharides, *A. aceti* ssp. *xylinum* synthesises a thick cellulosic pellicle which floats on the surface of the medium. Deep-etch freeze-fracture TEM reveals a densely packed network of apparently randomly oriented cellulose ribbons approximately 40 nm wide (Fig. 1 and Whitney et al. [26]).

Composites formed in the presence of Konjac glucomannan present a very different architecture (Fig. 2). The structure shows considerable heterogeneity, with very dense regions in which cellulose and glucomannan cannot be easily discerned, interspersed with areas in which cellulose ribbons can be distinguished, cross-linked by thinner strands consistent with single polysaccharide chains [26] and therefore attributed to glucomannan (Fig. 2a).

There is also evidence of a glucomannan network within a cellulose network (Fig. 2b).

The molecular organisation of cellulose–mannan composites was examined using  $^{13}\text{C}$  CP/MAS and SP/MAS NMR to probe relatively immobile and mobile chain segments respectively [36]. Konjac glucomannan composites have a greatly disrupted cellulose molecular organisation (Fig. 3a) compared to native bacterial cellulose (Fig. 3b and Table 3). Several additional signals appear as highfield shoulders on the C-1 peak of the composite compared to the control. There is a dramatic alteration in the crystalline:non-crystalline ratio for both C-4 (81–91 ppm) and C-6 (60–68 ppm) peaks. Integration of C-4 signals at ca. 88–91 and 84–86 ppm for crystalline and non-crystalline material respectively, gives a reduction in crystallinity from 80–85% to just 25%, concurring with the results of Hackney et al. [25].

Application of resolution enhancement to spectrum 3a (Fig. 3c) allows determination of the  $I\alpha/I\beta$  ratios by comparison of the C-4 crystalline signal with published quantified signal patterns [37,38]. A slight increase in the relative abundance of the  $I\beta$

crystalline form is revealed. The resolution enhanced spectrum also allows resolution of signals at ca. 101 ppm and ca. 103 ppm similar to those reported for mannosyl and glucosyl residues respectively for 30% glucomannan in water by Gidley et al. [32]. The signal intensity indicates that a significant proportion of glucomannan in the composite is relatively immobile, conferring visibility in the CP/MAS spectrum. These signals are also seen as the major C-1 signals in the SP/MAS spectrum of the same material (Fig. 3d). This split of visibility between the two spectra is as previously reported for glucomannan gels and hydrates [32]. The signal for C-1 of the glucosyl residue is overlapped by signals from non-crystalline cellulose at C-1.

An additional signal at ca. 102 ppm is seen (Fig. 3c), which is not visible in the SP/MAS spectrum (Fig. 3d). This shift is coincident with that for C-1 of the mannan I polymorph from ivory nut mannan [32,39] and is assigned here to C-1 of mannan structural units with an extended “cellulosic” conformation as found in crystalline mannan I [29,31]. Appearance of a

Table 1  
Monosaccharide composition of mannan additives

Sample	M:G <sup>a</sup>
Konjac glucomannan	1.63:1
Guar galactomannan	1.60:1
Fenugreek galactomannan	1.10:1
LBG <sub>uf</sub>	3.48:1
LBG <sub>25</sub>	2.91:1
LBG <sub>25–45</sub>	3.57:1
LBG <sub>45–80</sub>	5.58:1

<sup>a</sup> Ratio of mannose to glucose for Konjac glucomannan and mannose to galactose for the other mannan polysaccharides.

Table 2  
Monosaccharide composition of cellulose–mannan composites

Sample	Cellulose:Mannan	Man:Gal
0.5% Konjac glucomannan	1:0.59	n.d.
0.2% LBG <sub>uf</sub>	1:0.60	5.38:1
0.2% LBG <sub>25</sub>	1:0.43	4.49:1
0.2% LBG <sub>25–45</sub>	1:0.59	5.59:1
0.2% LBG <sub>45–80</sub>	1:1.34	6.64:1
0.5% LBG <sub>uf</sub>	1:1.19	5.52:1
0.5% LBG <sub>25</sub>	1:0.39	3.98:1
0.5% LBG <sub>25–45</sub>	1:0.54	5.76:1
0.5% LBG <sub>45–80</sub>	1:1.56	6.95:1
Guar gum	1:0.23	1.82:1
Fenugreek	1:0.16	1.10:1

Ratio of cellulose to gluco- or galactomannan for composites. Each result is the average of material isolated from three fermentations.  
n.d., not determined.

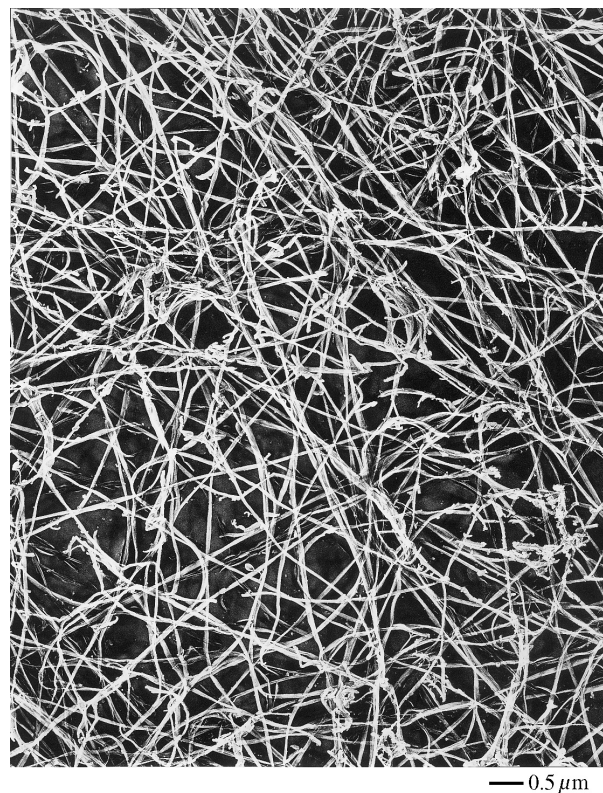


Fig. 1. Micrograph of tungsten/tantalum/carbon replica (printed in reverse contrast) of cellulose ribbons produced by *A. aceti* ssp. *xylinum* (ATCC 53524) showing an apparent random orientation and an underlying ribbon width of ca. 40 nm.

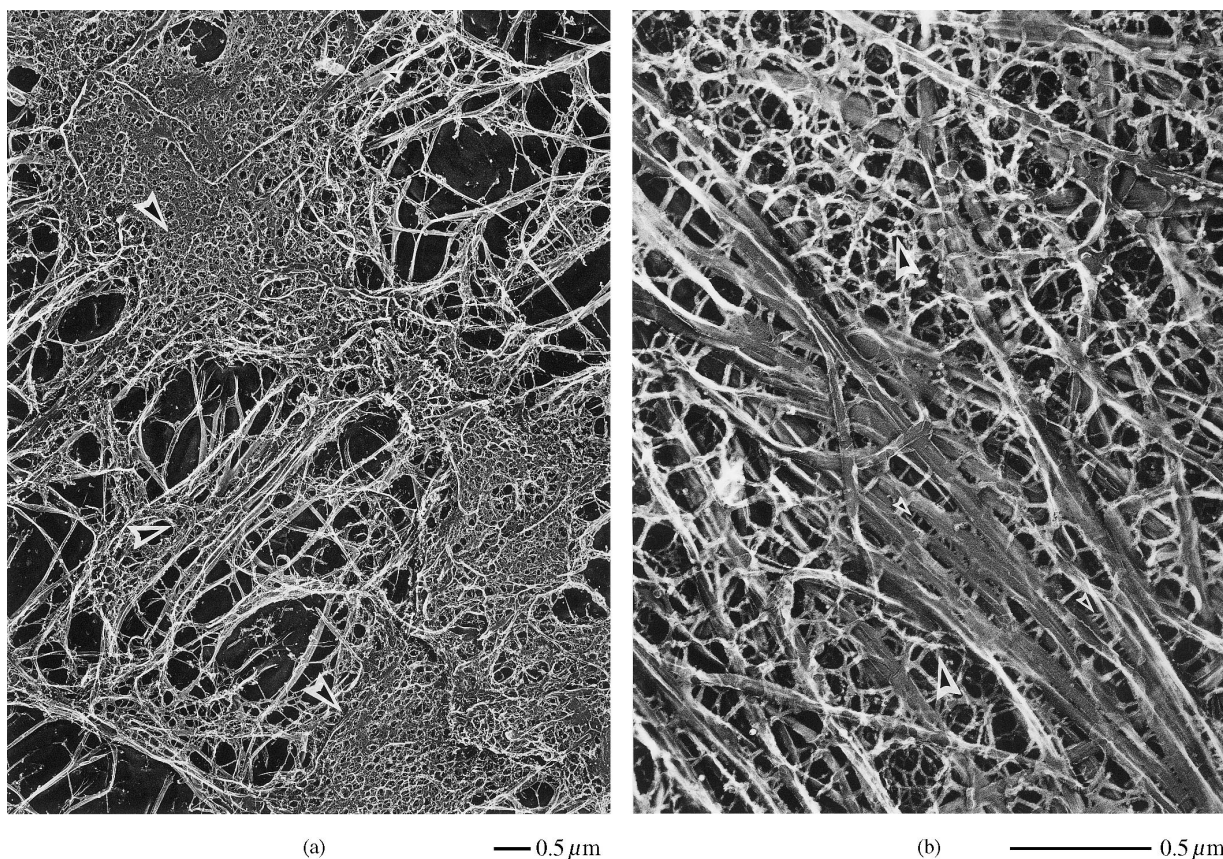


Fig. 2. Micrographs of a Konjac glucomannan composite. The structure is heterogeneous, with regions where cellulose and glucomannan cannot be readily distinguished (Fig. 2a, large arrows), regions of apparent cross-linking of cellulose ribbons by glucomannan (Fig. 2a and b, small arrows), and regions where a glucomannan network is apparently formed (Fig. 2b, large arrows).

signal at ca. 102 ppm was also observed by Kim and Newman [40] on mixing glucomannan with Avicel cellulose, and provides evidence for a conformational change of mannan segments upon association with cellulose. Any glucosyl residues in glucomannan which adopt a “cellulosic” conformation would be expected to have chemical shifts coincident with that of cellulose C-1 at 105–106 ppm and are therefore not detectable independently.

*Composites formed with galactomannan.*—The polydispersity of unfractionated LBG is apparent from calculation of Man:Gal ratios of fractions separated by differential solubility in water (Table 1). As predicted, the Man:Gal ratio increases with increasing temperature required for solubilisation [11,18]. Fenugreek galactomannan has the highest galactose content, with guar gum having an intermediate value between fenugreek and LBG<sub>25</sub>.

For all galactomannans, the general trend is for an increased level of incorporation into the cellulose composite with decreasing Gal content

(Table 2), providing some evidence for an interaction between cellulose and unsubstituted regions of the mannan backbone. There is very little association of the high Gal fenugreek and guar galactomannans with cellulose. Except for LBG<sub>uf</sub>, increasing the initial LBG concentration in the fermentation medium does not affect incorporation levels, indicating that LBG concentration is not a limiting factor. The dramatic increase in incorporation of LBG<sub>uf</sub> upon raising the initial concentration may be a reflection of the fact that 0.5% is significantly above the experimental entanglement concentration (determined as described by Morris et al. [41]) of 0.23%. At 0.2% there will be much less coil overlap (data not shown). An increased level of entanglement in unfractionated LBG may cause polymers which would otherwise not bind to cellulose (due to a low Man:Gal ratio) to be trapped by cellulose-high Man:Gal polymer networks. The presumed lower Man:Gal ratio polydispersity is proposed to make this mechanism inapplicable for fractionated LBG samples.

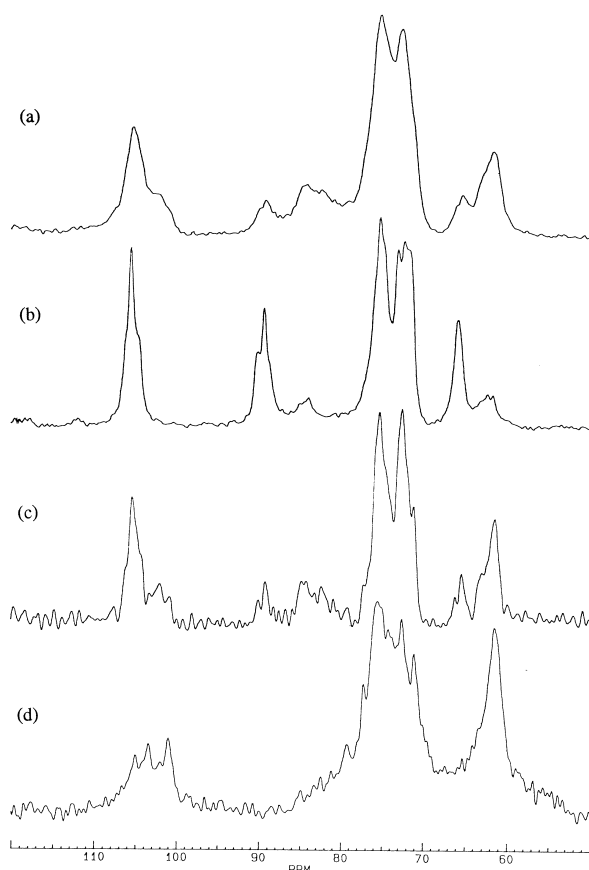


Fig. 3. NMR spectra of cellulose/glucomannan composite (a)  $^{13}\text{C}$  CP/MAS spectrum of the composite, (b) hydrated bacterial cellulose, (c) resolution enhancement (line broadening  $-70$  Hz, Gaussian multiplication 0.5) of (a), (d)  $^{13}\text{C}$  SP/MAS spectrum of the composite.

Comparing Man:Gal ratios of LBG fractions in the composite (Table 2) with the fractions as purified (Table 1), indicates positive selection for molecules with a higher mannose content within a

polydisperse population. This suggests cellulose–galactomannan interaction may be via the mannan backbone, and is consistent with the increased level of incorporation for low Gal materials.

Fenugreek galactomannan composites have network architectures predominantly similar to the controls with occasional zones apparently containing trapped galactomannan in a non-networked form (data not shown). Guar galactomannan composites have regions showing native cellulose architectures. However, there are also regions of randomly oriented cellulose fibres interspersed with a network of thinner strands attributed to guar galactomannan (Fig. 4). Although guar galactomannan shows many rheological features characteristic of entanglement networks [42], the concentration dependence of viscosity above the point of entanglement is steeper than for typical disordered polysaccharides [41] and there is a (reversible) decrease in viscosity on exposure to strong alkali [14]. This behaviour is considered to be due to some (limited) intermolecular association through regions of unsubstituted mannan [14,41]. Extending this concept, some intermolecular association between guar galactomannan and cellulose would also be predicted. Whether guar/guar or guar/cellulose interactions are responsible for the observed composite microstructure cannot be determined from the present data as the level of interaction is insufficient to cause any significant NMR-observable changes. The absence of regions containing a galactomannan network in fenugreek composites is more likely to be due to the lower Man:Gal ratio of fenugreek galactomannan (Table 1) rather than solution viscosities which were similar for the two materials.

Table 3  
Summary of  $^{13}\text{C}$  CP/MAS data for cellulose–mannan composites

Cellulose sample	Cellulose: GM ratio (from sugar anal.)	Cellulose: GM ratio in CP/MAS spectra	Cellulose $\text{I}\alpha/\text{I}\beta$ ratio	Cellulose molecular composition		
				$\text{I}\alpha$	$\text{I}\beta$	nc
Native bacterial cellulose	—	—	70:30	57%	25%	18%
0.5% konjac	1:0.59	*	60:40	15%	10%	75%
0.2% guar	1:0.23	*	70/30	45%	19%	36%
0.25% fenugreek	1:0.16	*	70/30	47%	20%	33%
0.2% LBG <sub>uf</sub>	1:0.60	1:0.48	70/30	41%	17%	42%
0.5% LBG <sub>uf</sub>	1:1.19	1:0.60	50/50	27%	26%	47%
0.2% LBG <sub>25</sub>	1:0.43	1:0.23	70/30	44%	19%	37%
0.5% LBG <sub>25</sub>	1:0.39	1:0.31	70/30	47%	20%	33%
0.2% LBG <sub>25-45</sub>	1:0.59	1:0.37	70/30	40%	17%	43%
0.5% LBG <sub>25-45</sub>	1:0.54	1:0.41	70/30	35%	15%	50%
0.2% LBG <sub>45-80</sub>	1:1.34	1:0.64	50/50	23%	22%	55%
0.5% LBG <sub>45-80</sub>	1:1.56	1:1.13	50/50	27%	26%	47%



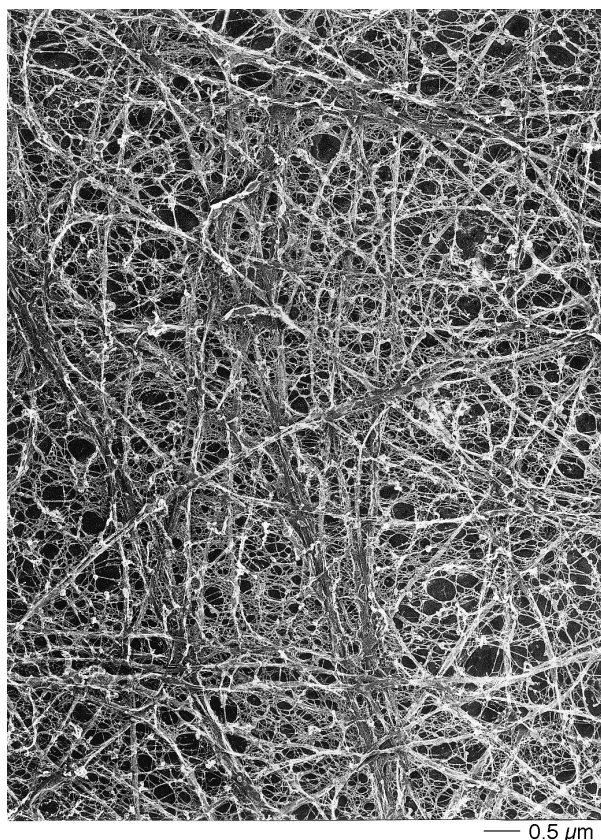


Fig. 4. Micrograph of a guar galactomannan composite showing an apparently randomly oriented network of cellulose fibres independent of a guar galactomannan network comprising single polysaccharide strands.

Composites formed in the presence of different LBG fractions show a range of architectural features (Fig. 5). LBG<sub>25</sub>-composites (Fig. 5a) present a cross-linked architecture. There is no evidence for the bulk cellulose fibre alignment seen in cross-linked xyloglucan composites [26] or for significant galactomannan self-association (contrast Fig. 5b). Most LBG<sub>25</sub> is apparently associated with cellulose, functioning as a cross-linking polysaccharide.

LBG<sub>45–80</sub> composites show a heterogeneity of architectural features. There is extensive self association of LBG (Fig. 5b) with structures consistent with those observed in LBG gels after freeze–thaw treatments [43], large scale cellulose ribbon alignment (Fig. 5c) and also apparently self-associated LBG in close proximity to cellulose fibres. LBG<sub>uf</sub> composites exhibit architectures with features of both LBG<sub>25</sub> and LBG<sub>45–80</sub>, and also show a concentration dependence of network architecture not seen with other LBG fractions. At low starting concentrations (0.2%), most of the LBG is visualised in association with cellulose (Fig. 5d). At 0.5%

starting concentration, much more self-association of LBG is apparent (Fig. 5e), with less evidence for association of cellulose ribbons. These data are consistent with the sugar analysis results, which showed a greatly increased LBG incorporation at higher starting concentrations of LBG<sub>uf</sub> (Table 2).

Cellulose molecular organisation is much less disrupted in all galactomannan composites compared to glucomannan (Table 3). Cellulose crystallinity is reduced but except for 0.5% LBG<sub>uf</sub> and LBG<sub>45–80</sub> fractions the I $\alpha$ /I $\beta$  ratio is identical to the control. Fenugreek galactomannan composites have no galactomannan signals in the CP/MAS spectrum (data not shown). All LBG- and guar-containing composites have signals at ca. 101.0 and 99.6 ppm in the CP/MAS spectrum, corresponding to mannosyl and galactosyl residues respectively of a native LBG gel [32] (Fig. 6). In addition, intensity at 102–103 ppm is also identified in all LBG-containing composites, coincident with that reported for mannosyl C-1 of mannan in an extended “cellulosic” conformation [39] and as seen in the cellulose/glucomannan composite. Upon resolution enhancement, two signals at ca. 102.5 and 102.8 ppm of approximately equal intensity are resolved (Fig. 6b and c).

Integration of signals at ca. 105 ppm corresponding to cellulose glucosyl C-1, mannose C-1 signals at ca. 102.5 and 101 ppm and the galactose C-1 signal at ca. 99.6 ppm allows calculation of cellulose:galactomannan ratios in CP/MAS spectra (Table 3). A significant proportion of total galactomannan in all composites is visible in the SP/MAS spectrum (e.g., Fig. 6e). Resonances for mannosyl and galactosyl C-1 of LBG are identical in SP/MAS and CP/MAS spectra, as described by Gidley et al. [32]. In particular, the increase in galactomannan visible in CP/MAS spectra of composites from 0.2% to 0.5% concentration is no greater for the unfractionated sample than for fractions. This suggests that the extra galactomannan incorporated from 0.5% LBG<sub>uf</sub> is trapped within the structure rather than associated with cellulose.

There is a general trend of increased self association of LBG for higher Man galactomannans ie increased signal intensity at ca. 101 and 99.6 ppm corresponding to LBG gel/hydrate, relative to that at ca. 102.5 ppm corresponding to the mannan I conformation (compare Fig. 6a with b). As predicted [32], there is relative enrichment of the LBG gel mannosyl C-1 signal in CP/MAS compared to

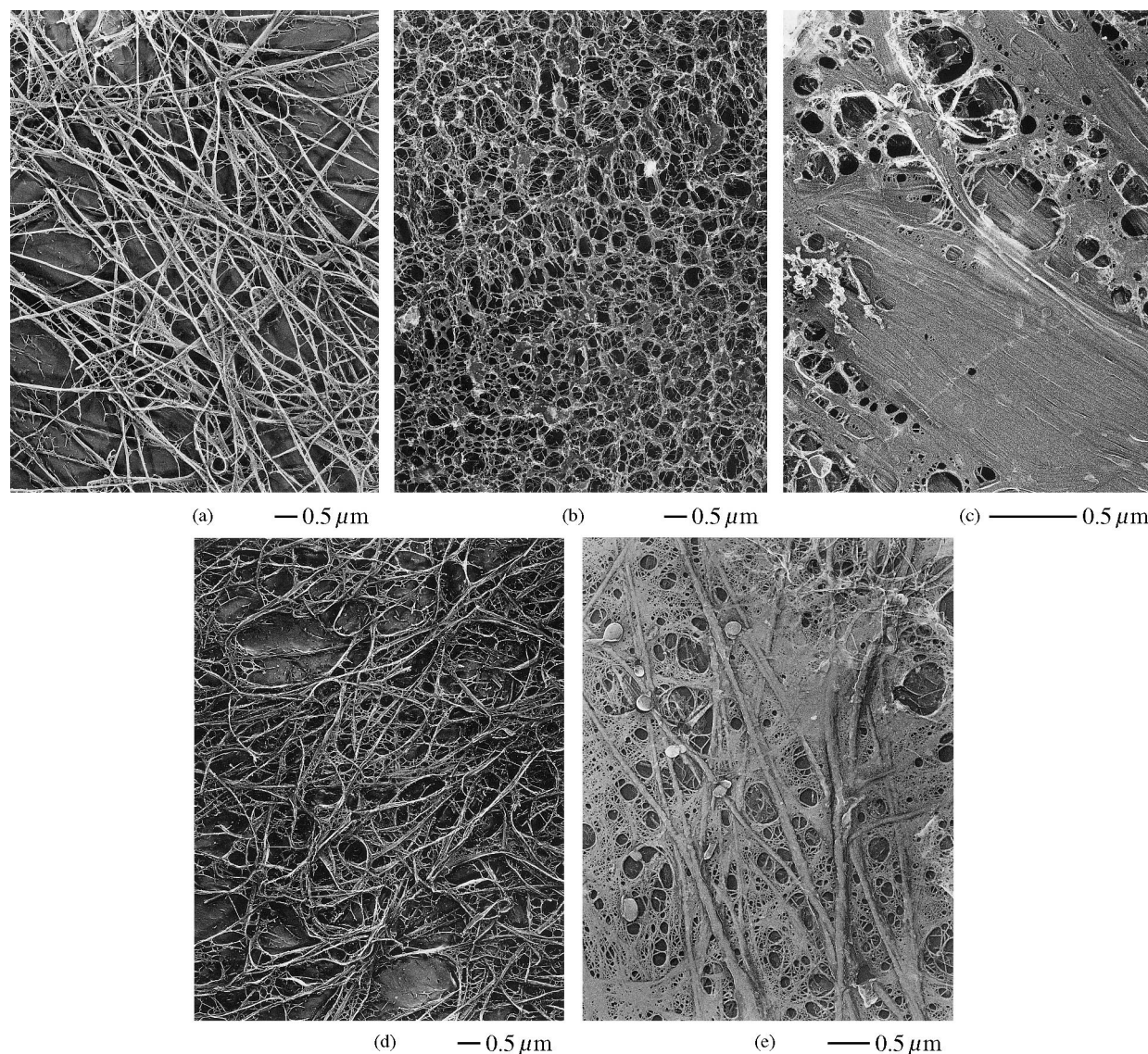


Fig. 5. Micrographs of composites produced with a range of LBG fractions: (a) 0.2% LBG<sub>25</sub> composite showing that the predominant effect is cross-linking of cellulose ribbons; lower Gal galactomannans such as 0.2% LBG<sub>45–80</sub> give very different structures with evidence for LBG gel formation (b) as well as cellulose ribbon alignment (c); (d) shows structures formed with 0.2% LBG<sub>uf</sub>, with cross-linking of cellulose by single polysaccharide strands assumed to be LBG being the predominant effect; (e) at the higher starting concentration of 0.5%, LBG<sub>uf</sub> shows significant self association.

that in the SP/MAS spectrum. Enrichment in high mannose LBG in composites as revealed by monosaccharide analysis (Table 1) can be attributed mainly to relatively immobile Man residues ie mannan-rich regions involved in either gel formation or cellulose binding.

#### 4. Discussion

*Cellulose/glucomannan interactions.*—Glucomannan is mainly described as a major hemicellulose polymer in secondary cell walls, but is

often reported as forming part of Type I primary cell walls (e.g., ref. [7]). Konjac glucomannan forms highly heterogeneous structures with *Acetobacter* cellulose (Fig. 2). Of interest is the apparent ability of glucomannan to cross-link cellulose ribbons. For Type I cell walls, xyloglucan is traditionally regarded as the major cross-linking hemicellulose, imparting lateral organisation to cellulose microfibrils within the cell wall [6,44]; in those primary cell walls which contain (galacto)glucomannan in significant quantities, xyloglucan may not necessarily be the only polymer cross-linking the cellulose network.



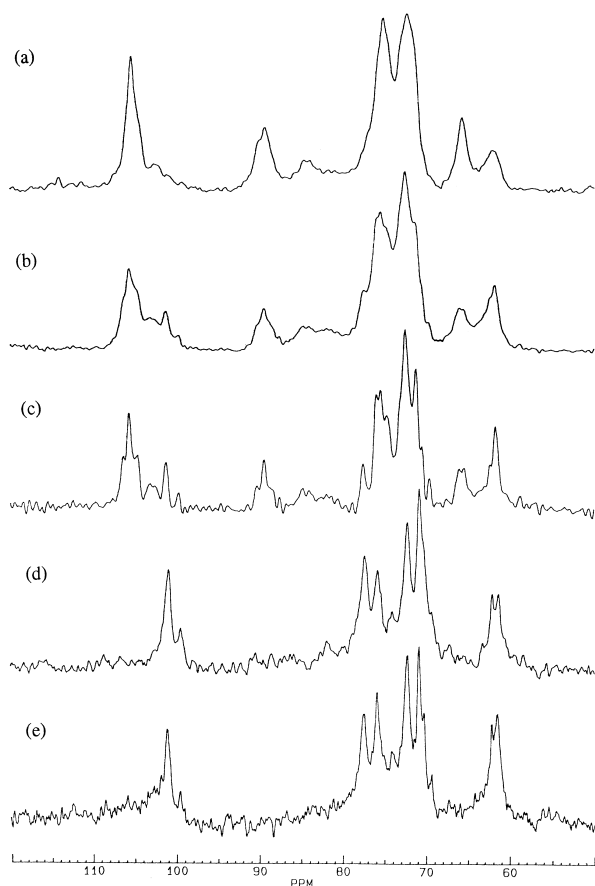


Fig. 6.  $^{13}\text{C}$  CP/MAS NMR spectra of cellulose/galactomannan composites (a) composites formed in presence of 0.5% LBG<sub>25</sub> and (b) 0.2% LBG<sub>45–80</sub>; (c) after application of resolution enhancement (line broadening  $-70\text{ Hz}$ , Gaussian multiplication 0.5) to spectrum (b); (d)  $^{13}\text{C}$  SP/MAS spectrum of native LBG gel; (e)  $^{13}\text{C}$  SP/MAS spectrum of cellulose/LBG<sub>45–80</sub> composite.

Glucomannan is thought to have no block mannan or cellulosic structures [10]. After deacetylation, Konjac glucomannan can be induced to form gels in which signals at ca. 101.1 ppm and 103.8 ppm corresponding to mannosyl and glucosyl C-1 respectively, can be identified [32]. These authors reported relative enrichment of the glucosyl resonance in the gel compared to the hydrate, implying glucan-enriched junction zones. Neither the mannan I or cellulose I/II conformation is reported in glucomannan gels [32], but the mannan I C-1 signal at ca. 102.5 ppm can be clearly identified in cellulose/glucomannan composites (Fig. 3), in addition to the predicted signal for non-ordered mannan at ca. 101 ppm. Cellulose apparently acts as a template resulting in a proportion of the Man residues in glucomannan adopting a “cellulosic” conformation. A further inference is that extended

2-fold “cellulosic” conformations are not a significant component in gels of either glucomannan or galactomannan.

As had previously been shown [25], cellulose synthesised in the presence of Konjac glucomannan has drastically reduced overall crystallinity, with little effect on the nature of the remaining crystalline component (Table 3). The effect is much more pronounced than is seen with galactomannans, even when comparing samples with equivalent cellulose/mannan ratios (e.g., cellulose/glucomannan compared with cellulose/0.2% LBG<sub>uf</sub>). Konjac glucomannan has a low degree of side chain (primarily acetate) substitution [10]; the only galactomannan fractions which significantly perturbed cellulose molecular organisation were the low galactose LBG<sub>45–80</sub> and 0.5% LBG<sub>uf</sub>. Mannans with a low level of side chain substitution are apparently more effective at disrupting cellulose organisation, indirect evidence for intimate mannan-cellulose interactions at the molecular level.

Reduction in cellulose crystallinity from 80–85% to 25% shows that most of the cellulosic chains are perturbed by the presence of glucomannan. Cellulose fibrils are at least as wide in the glucomannan composites as in the native cellulose, implying that much of the glucomannan is present within fibrils.

*Cellulose/galactomannan interactions.*—Both self-association and association of galactomannans with other polysaccharides is positively correlated with decreasing Gal content [13,15,19]. A significant effect of galactomannan fine structure is also reported, with interactions enhanced when the fine structure has blocks of unsubstituted mannose available [13]. For galactomannan composites the general trend is as predicted i.e. greater incorporation for low Gal galactomannans, and a selection for low Gal species upon incorporation (Table 2, c.f. Table 1). The perturbation of cellulose molecular organisation also follows the same trend (Table 3), implying that galactosyl substitution presents a significant barrier to incorporation within cellulose fibrils.

LBG-cellulose composites contain three structural features. Firstly, a component intimately associated with cellulose in which the mannan backbone adopts the extended cellulosic conformation. Secondly, a relatively immobile LBG fraction. Although at the concentrations and incubation conditions used, LBG will not form a gel network in isolation, it is possible that the localised

concentration of LBG within a constraining cellulose framework may induce gel formation, as is seen with the freeze–concentration effect which facilitates LBG gel formation by freeze–thawing [15,45]. Ultrastructurally, this fraction is similar to freeze–thaw induced LBG gels [43]. Thirdly, a significant proportion of incorporated LBG is relatively mobile within the composite. In addition to segments trapped within LBG networks, this is assigned to LBG involved in cross-linking adjacent cellulose fibres (Fig. 5a and d), analogous to a relatively mobile xyloglucan fraction in cellulose/xyloglucan composites [26].

The presence of cross-links could either reflect structural features within galactomannans which limit/prevent cellulose association, entrapment of segments adjacent to regions bound to different cellulose fibrils (kinetic control), or adoption of a lowest free energy state with entropic contributions from cross-links (thermodynamic control). The latter explanation was proposed for the cellulose/xyloglucan interaction, in which formation of regularly sized cross-linkages by the homogeneous and highly substituted tamarind xyloglucan was best explained solely by entropy/enthalpy arguments [26]. Galactomannans have a much more polydisperse fine structure than tamarind xyloglucan [6,13] so limitations of cellulose binding by highly substituted regions may explain the irregularity in cross-link dimensions observed. One consequence of this irregularity is that, unlike xyloglucan [26] long range alignment of fibrils is not pronounced.

For lower Gal contents (LBG<sub>45–80</sub>) bulk cellulose fibre coalescence (Fig. 5c) as well as LBG gel formation (Fig. 5b) is observed. As direct interactions between cellulose ribbons are not seen in the absence of added polymers, we propose that fibre alignment occurs through relatively unbranched mannan segments binding to two or more cellulose fibres.

*Comparison with xyloglucan and implications for cell wall assembly.*—Assembly of the cellulose/hemicellulose framework of plant cell walls [6] can be conceptualised as a hierarchical self-assembly process [46]. Adding different hemicelluloses to the *Acetobacter* system gives altered architectural and molecular features (ref. [26] and this paper) suggesting that the type(s) of hemicellulose present at the site of cellulose synthesis may determine the nature of the cell wall laid down around the cell. Xyloglucan, the hemicellulose associated with Type

I [6] primary cell walls, gives a highly ordered network architecture with *Acetobacter* cellulose [26]. Cellulose fibres are cross-linked by xyloglucan and these cross-linkages are highly conserved in length, a feature which may be related to the regular sub-unit structure of the tamarind xyloglucan used [26] but which is also seen in Type I primary cell walls [44].

Networks synthesised in the presence of gluco- or galactomannans are shown to have distinct architectural and molecular features. A wide range of cross-link lengths are obtained and cellulose fibril coalescence is seen in the presence of mannan with a low level of sidechain substitution. Gluco- and galactoglucomannan structures are found in many plant cell walls. Our results show that, by tailoring the levels of Gal and Glu incorporation, a range of cellulose-associated networks could be formed. In Type I primary cell walls which contain mannan-based polymers, cross-linkages need not be uniquely associated with xyloglucans. In secondary cell walls, gluco- and galactoglucomannans are often major components. Significant fibril coalescence in composites of glucomannan and low Gal galactomannans (Figs. 2 and 5) in the high dilution conditions used in this work may represent a natural function of these polymers. In secondary cell walls, cell growth is no longer occurring and a primary requirement is for strength. This could be achieved by coalescence/densification of cellulose resulting in the expulsion of water. Mannan-based polymers appear to possess this capability. In contrast, primary walls must have the ability to expand as cells grow: this implies a degree of flexibility requiring a highly hydrated environment. Xyloglucan–cellulose networks can achieve this through spacing of fibrils via xyloglucan crosslinks.

## References

- [1] H. Meier and J.S.G. Reid, *Encycl. Plant Physiol. New. Ser.*, 13A (1982) 418–471.
- [2] E. Frei and R.D. Preston, *Proc. Roy. Soc. B*, 169 (1968) 127–145.
- [3] J.S.G. Reid, *Adv. Bot. Res.*, 11 (1985) 125–155.
- [4] M. Edwards, C. Scott, M.J. Gidley, and J.S.G. Reid, *Planta*, 187 (1992) 67–74.
- [5] J.S.G. Reid, M. Edwards, M.J. Gidley, and A.H. Clark, *Planta*, 195 (1995) 489–495.
- [6] N.C. Carpita and D.M. Gibeaut, *Plant J.*, 3 (1993) 1–30.

- [7] G.B. Seymour, I.J. Colquhoun, M.S. DuPont, K.R. Parsley, and R.R. Selvendran, *Phytochemistry*, 29 (1990) 725–731.
- [8] P. Ryden and R.R. Selvendran, *Biochem. J.*, 269 (1990) 393–402.
- [9] P. Ryden and R.R. Selvendran, *Carbohydr. Res.*, 195 (1990) 257–272.
- [10] K. Nishinari, P.A. Williams, and G.O. Phillips, *Food Hydrocolloids*, 6 (1992) 199–222.
- [11] I.C.M. Dea and A. Morrison, *Adv. Carbohydr. Chem. Biochem.*, 31 (1975) 241–312.
- [12] B.V. McCleary, I.C.M. Dea, J. Windust, and D. Cooke, *Carbohydr. Polym.*, 4 (1984) 253–270.
- [13] I.C.M. Dea, A.H. Clark, and B.V. McCleary, *Carbohydr. Res.*, 147 (1986) 275–294.
- [14] F.M. Goycoolea, E.R. Morris, and M.J. Gidley, *Carbohydr. Polym.*, 27 (1995) 69–71.
- [15] I.C.M. Dea, E.R. Morris, D.A. Rees, E.J. Welsh, H.A. Barnes, and J. Price, *Carbohydr. Res.*, 57 (1977) 249–272.
- [16] P. Cairns, M.J. Miles, V.J. Morris, and G.J. Brownsey, *Carbohydr. Res.*, 160 (1987) 411–423.
- [17] P. Annable, P.A. Williams, and K. Nishinari, *Macromolecules*, 27 (1994) 4202–4211.
- [18] R.O. Mannion, C.D. Melia, B. Launay, G. Cuvelier, S.F. Hill, S.E. Harding, and J.R. Mitchell, *Carbohydr. Polym.*, 19 (1992) 91–97.
- [19] L. Lundin and A.-M. Hermansson, *Carbohydr. Polym.*, 28 (1995) 91–99.
- [20] F.M. Goycoolea, R.K. Richardson, E.R. Morris, and M.J. Gidley, *Biopolymers*, 36 (1995) 643–658.
- [21] C.H. Haigler, R.M. Brown Jr., and M. Benziman, *Science*, 210 (1980) 903–906.
- [22] M. Benziman, C.H. Haigler, R.M. Brown Jr., A.R. White, and K.M. Cooper, *Proc. Natl Acad. Sci. USA*, 77 (1980) 6678–6682.
- [23] C.H. Haigler, A.R. White, R.M. Brown Jr., and K.M. Cooper, *J. Cell. Biol.*, 94 (1982) 64–69.
- [24] R.H. Atalla, J.M. Hackney, I. Uhlin, and N.S. Thompson, *Int. J. Biol. Macromol.*, 15 (1993) 109–112.
- [25] J.M. Hackney, R.H. Atalla, and D.L. van der Hart, *Int. J. Biol. Macromol.*, 16 (1994) 215–218.
- [26] S.E.C. Whitney, J.E. Brigham, A.H. Darke, J.S.G. Reid, and M.J. Gidley, *Plant J.*, 8 (1995) 491–504.
- [27] H. Yamamoto and F. Horii, *Cellulose*, 1 (1994) 57–66.
- [28] K.T. Uhlin, R.H. Atalla, and N.S. Thompson, *Cellulose*, 2 (1995) 129–144.
- [29] H.D. Chanzy, A. Grosrenaud, J.P. Joseleau, M. Dube, and R.H. Marchessault, *Biopolymers*, 21 (1982) 301–319.
- [30] Y.Y. Chien and W.T. Winter, *Macromolecules*, 18 (1985) 1357–1359.
- [31] H. Chanzy, S. Perez, D.P. Miller, G. Paradossi, and W.T. Winter, *Macromolecules*, 20 (1987) 2407–2413.
- [32] M.J. Gidley, A.J. McArthur, and D.R. Underwood, *Food Hydrocolloids*, 5 (1991) 69–40.
- [33] J.M.A. Campbell and J.S.G. Reid, *Planta*, 155 (1982) 105–111.
- [34] S. Hestrin and M. Schramm, *Biochem. J.*, 58 (1954) 345–352.
- [35] A.B. Blakeney, P.J. Harris, R.J. Henry, and B.A. Stone, *Carbohydr. Res.*, 113 (1983) 291–299.
- [36] T.J. Foster, S. Ablett, M.C. McCann, and M.J. Gidley, *Biopolymers*, 39 (1996) 51–56.
- [37] E.M. Debzi, H. Chanzy, J. Sugiyama, P. Tekeley, and G. Excoffier, *Macromolecules*, 24 (1991) 6816–6822.
- [38] H. Yamamoto and F. Horii, *Macromolecules*, 26 (1993) 1313–1317.
- [39] R.H. Marchessault, M.G. Taylor, and W.T. Winter, *Can. J. Chem.*, 68 (1990) 1192–1195.
- [40] T.S. Kim and R.H. Newman, *Holzforschung*, 49 (1995) 109–114.
- [41] E.R. Morris, A.N. Cutler, S.B. Ross-Murphy, D.A. Rees, and J. Price, *Carbohydr. Polym.*, 1 (1981) 5–21.
- [42] R.K. Richardson and S.B. Ross-Murphy, *Int. J. Biol. Macromol.*, 9 (1987) 250–256.
- [43] J.E. Brigham, M.J. Gidley, R.A. Hoffmann, and C.G. Smith, *Food Hydrocolloids*, 8 (1994) 331–344.
- [44] M.C. McCann, B. Wells, and K. Roberts, *J. Cell Sci.*, 96 (1990) 323–334.
- [45] H. Maier, M. Anderson, C. Karl, K. Magnuson, and R.L. Whistler, in R.L. Whistler and J.N. BeMiller (Eds.), *Industrial Gums*, 3rd edn, Academic Press, San Diego, 1993, pp. 181–226.
- [46] R.M. Brown, *J. Macromol. Sci.—Pure Appl. Chem.*, A33 (1996) 1345–1373.